IEEE Access
Multidisciplinary | Rapid Review | Open Access Journal

Received December 3, 2019, accepted December 29, 2019, date of publication January 6, 2020, date of current version January 17, 2020.

Digital Object Identifier 10.1109/ACCESS.2020.2963988

Influence of Fluorescence to Photon Lifetime Ratio on Detection Sensitivity in Laser Self-Mixing Interferometry

KE KOU, CUO WANG, AND JUN WENG
School of Mechanical and Precision Instrument Engineering, Xi'an University of Technology, Xi'an 710048, China
Corresponding author: Ke Kou (kouke881101@tju.edu.cn)

This work was supported in part by the National Natural Science Foundation of China under Grant 61803302 and Grant 61803299, in part by the Natural Science Foundation of Shaanxi Province under Grant 2017JQ6062, and in part by the Scientific Research Program Funded by Shaanxi Provincial Education Department under Grant 17JK0540 and Grant 19JK0589.

ABSTRACT Laser self-mixing interferometry (SMI) has been widely applied in the fields of precision measurement in scientific research, industry and biomedicine, and most researchers preferentially utilize laser diodes (LD) as light sources due to their compact structure and low cost. In most SMI cases, detection sensitivity rather than structure and cost is always the first concern. So in this article, we concentrate on an influencing factor on detection sensitivity named fluorescence to photon lifetime ratio (FPLR) which is an inherent parameter of the active material in a laser cavity. Derivation and simulation based on the time delayed rate equations are followed to validate the significant role played by the FPLR, then experiments according to different laser types including solid state lasers (SSL) and LDs are implemented to further prove the factor mentioned. Results demonstrate that SSLs always have higher detection sensitivity to feedback light than LDs, and is always more suitable to be applied in precision measurement. Additionally, the Yb:YAG laser is more sensitive than the Nd:YAG one. Increasing the pumping level from the threshold will decrease the SMI signal's sensitivity, and reducing laser feedback strength will also decrease the SMI signal's sensitivity. The findings from this article are beneficial to studying laser feedback sensitivity and selecting appropriate laser types in designing SMI sensors or instruments. Though with the disadvantages of large size and high cost, SSLs may be more suitable light sources in the field of high performance SMI sensing if miniaturization and cost are not the significant consideration.

INDEX TERMS Laser self-mixing interferometry, fluorescence to photon lifetime ratio, sensitivity, solid state laser, laser diode.

I. INTRODUCTION

As an emerging optical technique during the last several decades, laser self-mixing interferometry (SMI) has always attracted lots of attentions from institutes worldwide [1]. Laser diodes (LD) are always the first choices when implementing SMI measurement mainly because of miniature configuration, low cost and easy detection with built-in photodiodes (PD) [2], [3]. Till now, LD based SMI has been widely applied in the sensing fields covering displacement, distance, velocity, imaging, particle sizing and laser characteristics such as feedback strength factor, line-width enhancement factor and free spectral range [4]. It is a common case in the domain of precision measurement that sensing sensitivity rather than compact structure is researchers' main concern. Therefore, LDs may not be the most suitable laser sources, and concentration may has been turned from LDs to solid-state lasers (SSL), primarily due to their large fluorescence-to-photon lifetime ratio (FPLR), which has been reported to have influence on detection sensitivity [5]. Laser type selection may become the first problem encountered when developing SMI sensors or instruments.

Regarding laser types, different researchers have their own inclination. Donati and Norgia [6], Usman *et al.* [7] and Guo *et al.* [8] have always preferred to employ LDs to do SMI measurement or to study relevant phenomena. Liang Lu from Anhui university has been the supporter of fiber lasers [9], [10]. He-Ne lasers have sometimes been utilized [11],

The associate editor coordinating the review of this manuscript and approving it for publication was Md. Selim Habib.

much less frequently than other laser types. Kenju Otsuka is a forerunner to introduce SSLs to the field of SMI [12]. Then, Shulian Zhang's team from Tsinghua university began to devote plenty of time to SSL based SMI [13]–[15]. They have always underlined the significance of the FPLR in enhancing detection sensitivity [5], but thorough theoretical analysis and corresponding experiment validation have rarely been reported. The paper mainly concerns about SSLs and LDs, and compare their FPLR and detection sensitivity when illuminating external targets.

The paper is organized as follows. Next part focuses on the theoretical background of the FPLR and supplies relevant simulation results in both frequency and time domains. Then, some experiments based on different laser types are conducted to serve as practical validation. Finally, Conclusion is followed to tie the whole article together and provide some suggestions for selecting a suitable laser type for SMI sensors.

II. THEORETICAL ANALYSIS AND SIMULATION

Considering detection sensitivity is highly dependent on signal-to-noise ratio (SNR), typical and simple SMI Doppler signals with external rotating targets are employed to analyze the concerned sensitivity performance. The resultant Doppler frequency f_D is easily presented in Eq. (1) [16], [17].

$$f_D = 2\omega_r r \cos\theta/\lambda \tag{1}$$

where ω_r is the rotational speed measured in radians, r is the distance between the laser spot and the axis of the rotating disc, θ is the incident angle between the moving direction of the target and the optical axis, and λ is the wavelength of the laser. If the Doppler frequency approaches the relaxation oscillation frequency (ROF) of the laser, the SNR can be gradually promoted and then the sensitivity is further enhanced.

Detailed analysis about the sensitivity is correlated with lasers' dynamic behavior which can be described by the famous time-delayed Lang-Kobayashi equations [18]. Considering only the power spectrum of the slow-varying electric field is discussed and the characteristics of the frequency spectrum of the electric field itself is out of the scope of this article, the phase equation can be omitted for simplification, as shown in Eq. (2) [14].

$$\begin{cases} \dfrac{dN(t)}{dt} = \gamma_1 N_0 - \gamma_1 N(t) - BN(t)|E(t)|^2 \\ \dfrac{dE(t)}{dt} = \dfrac{1}{2}\left[BN(t) - \gamma_c\right]E(t) \\ \qquad\qquad +\gamma_c\gamma_{ext}\cos\left[\Omega t - (\omega+\Omega)\tau\right]E(t) \end{cases} \tag{2}$$

where $N(t)$ is the population inversion, $E(t)$ is the amplitude of the laser electric field whose square is the laser intensity in photon unit, ω is the laser's angular frequency, and Ω is the shifted Doppler frequency in the angular form. γ_1 and γ_c are the decay rates of the population inversion and the laser cavity, respectively, which are the reciprocals of the fluorescence lifetime and the photon lifetime, and γ_c/γ_1 indicates the FPLR proposed. $\gamma_1 N_0$ is the pumping rate. B is the Einstein coefficient, which is the product of laser speed in air c and the cross section area of the stimulated emission in the laser material σ. γ_{ext} is the laser feedback coefficient, and τ is the round-trip delayed time of the external target.

The stationary solutions of Eq. (2) without laser feedback is easily obtained.

$$\begin{cases} N_s = \dfrac{\gamma_c}{B} \\ I_s = |E_s|^2 = \dfrac{\gamma_1}{B}(\eta - 1) \end{cases} \tag{3}$$

where $\eta = N_0/N_s = N_0\, B/\gamma_c$ is the normalized pumping rate.

$N(t)$ and $E(t)$ can be written as Eq. (4).

$$\begin{cases} N(t) = N_s(1+\Delta n) \\ E(t) = I_s(1+\Delta e) \end{cases} \tag{4}$$

where Δn and Δe are the relative perturbation corresponding to their stationary values N_s and E_s. Substituting (4) into (2) and neglecting all the second-order terms including $\Delta n\Delta e$, Δn^2, or Δe^2, the final equations to be analyzed can be described as Eq. (5).

$$\begin{cases} \dfrac{d\Delta n}{dt} = -\gamma_1\eta\Delta n - 2\gamma_1(\eta-1)\Delta e \\ \dfrac{d\Delta e}{dt} = \dfrac{1}{2}\gamma_c\Delta n + \gamma_c\gamma_{ext}\cos\left[\Omega t - (\omega+\Omega)\tau\right] \\ \qquad\qquad +\gamma_c\gamma_{ext}\cos\left[\Omega t - (\omega+\Omega)\tau\right]\Delta e \end{cases} \tag{5}$$

Since there are no analytical solutions of Eq. (5), its numerical ones can be derived from an iteration methodology shown in Eq. (6).

$$W_{i+1} = W_i + F(W_i)\Delta t, \quad W = \Delta n,\ \Delta e. \tag{6}$$

where Δt means the step size, and F indicates the right-side terms of Eq. (5). Smaller step size generally indicates larger computational cost and more accurate results.

A. SIMULATION IN FREQUENCY DOMAIN

Totally three different lasers, a Nd:YAG SSL, a Yb:YAG SSL and a LD, are employed to analyze sensitivity under the same Doppler frequency shifting which is easily introduced by an external rotating or linearly moving target. All the simulation parameters are summarized in the following Table 1.

All the numerical simulations are implemented by Python 3.7, relying on the numpy package to provide numerical methods, the matplotlib package to plot figures, and the numba package to accelerate the calculation process.

The power spectra of these two SSLs are presented in Fig. 1. The pumping rate values in these two SSLs are adjusted to make the ROF be the same to ensure a common frequency response. The Doppler peak of the Yb:YAG is about 3 dB higher than that of the Nd:YAG, as predicted from the fact that the FPLR of the Yb:YAG is larger than that of the Nd:YAG. Additionally, a higher feedback coefficient always indicates a higher power spectrum, but the power differences between these two SSLs nearly hold stationary

TABLE 1. Simulation parameters of three laser types.

Parameter	Yb:YAG	Nd:YAG	LD
γ_1	$1/(270\times10^{-6})\ s^{-1}$	$1/(90\times10^{-6})\ s^{-1}$	$1/(2\times10^{-9})\ s^{-1}$
γ_c	$1/(176\times10^{-12})\ s^{-1}$	$1/(235\times10^{-12})\ s^{-1}$	$1/(2\times10^{-12})\ s^{-1}$
$\gamma_1 N_0$	$1.2\times10^{27}\ s^{-1}m^{-3}$	$2.2\times10^{27}\ s^{-1}m^{-3}$	$1.15\times10^{34}\ s^{-1}m^{-3}$
λ	1030 nm	1064 nm	850 nm
ω	1.83×10^{15} rad/s	1.77×10^{15} rad/s	2.22×10^{15} rad/s
FPLR	1.53×10^{6}	3.83×10^{5}	10^{3}
B		$2.64\times10^{-14}\ m^3/s$	
γ_{ext}		1×10^{-6}, 5×10^{-6} and 1×10^{-5}	
Ω		$2\pi\times3\times10^{5}$ rad/s	
τ		0.7 ns	
Δt		0.01 n	

as the feedback coefficient changes. Obviously, the spectrum under higher feedback level tends to exhibit harmonic peaks or parametric peaks, as reported in [14].

The power spectra of the LD under different feedback coefficients is shown in the following Fig. 2. The power spectra look quite similar except power difference, and the ROF peaks of the LD appear around GHz level, far away from those in SSLs. Therefore, the SNR enhancement in LDs caused by general Doppler peak can be negligible when compared with SSLs.

It can be concluded from the these results that SSLs always have higher sensitivity to optical feedback than LDs due to their pronounced difference in the FPLR which can be up to several orders of magnitude, and in the field of SSLs, the Yb:YAG can be somewhat more sensitive than the Nd:YAG for the similar reason.

B. SIMULATION IN TIME DOMAIN

Unlike frequency analysis above, time domain observation is more convenient to be applied to validate the sensitivity. As shown in the typical SMI power equation in Eq. (7), P_0 and ΔP are the direct and alternating components of the SMI signal, respectively, and ϕ_F is the phase term under laser feedback [19], [20].

$$P = P_0 + \Delta P = P_0\,[1 + m\cos(\phi_F)] \tag{7}$$

P_0 indicates the power level, and the quotient of ΔP and P_0 is shown in Eq. (8).

$$\Delta P/P_0 = m\cos(\phi_F) \tag{8}$$

The amplitude m or the peak-to-peak value $2m$ can be adopted to characterize the sensitivity performance. Obviously, under the same operating condition, larger amplitude indicates higher sensitivity. For a segment of a SMI signal, itself can be regarded as P and its mean value corresponds to P_0. The sensitivity indicator m or $2m$ can be easily obtained. Comparing Eq. 4 and Eq. 7, Δe corresponds to the term $m\cos(\phi_F)$ here, and the peak-to-peak amplitude $2m$ can be utilized for subsequent analysis.

All the parameters listed in Table 1 are adopted in time domain simulation, except that the shifting frequency Ω is changed to $2\pi\times1\times10^4$ rad/s (10 kHz) as the Doppler frequency caused by the target in the experiments will be no more than 10 kHz and the pumping rate $\gamma_1 N_0$ of each laser type is changed to 1.1, 1.2, 1.3 and 1.4 times of the threshold one. All the numerical simulations are also implemented by Python 3.7, and the results are demonstrated in following Fig. 3. It can be easily observed that for all three laser types, the sensitivity reduces as the relative pumping rate increases and as the feedback level decreases. Higher pumping rate moves the ROF peak more far away from the Doppler peak (10 kHz here), inducing less enhanced signals and smaller $2m$ values. Less amount of feedback light coupled into the laser cavity definitely produces smaller signals. Of course, due to the difference in the FPLR, SSLs always have higher sensitivity to optical feedback than LDs, and the Yb:YAG is also more sensitive than the Nd:YAG, which coincides with the simulation results in frequency domain.

III. EXPERIMENTAL VALIDATION

The Experimental setup utilized to validate the concept mentioned above is depicted in the following Fig. 4.

Two microchip SSLs are adopted, one with the laser crystal of Nd:YAG and another with Yb:YAG. Both of them have round shapes with the diameter of 10 mm and the thickness of 0.75 mm. The differences exist in doping concentration and coating. The Nd:YAG one shows the doping concentration of 1.2% while the Yb:YAG one shows that of 15%. The pumping facet of the Nd:YAG one is coated by a high transmittance film at 808 nm and a high reflectance film at 1064 nm, and the emitting facet is coated by a high reflectance film at 808 nm and a 5% transmittance film at 1064 nm. While in the Yb:YAG, the pumping facet is coated by a high transmittance film at 940 nm and a high reflectance film at 1030 nm, and the emitting facet is coated by a high reflectance film at 940 nm and a 5% transmittance film at 1030 nm. Furthermore, a vertical cavity surface emitting laser (VCSEL), belonging to LD family, is also used to make the whole experiment more complete. It has the threshold current of 2 mA and the general output power of 2 mW. A neutral density filter (NDF), with a rectangular shape and a gradually decreasing transmittance along one side, is inserted in the configuration to adjust the feedback strength. The external target is a PZT stage (Thorlabs, PE4) driven by a

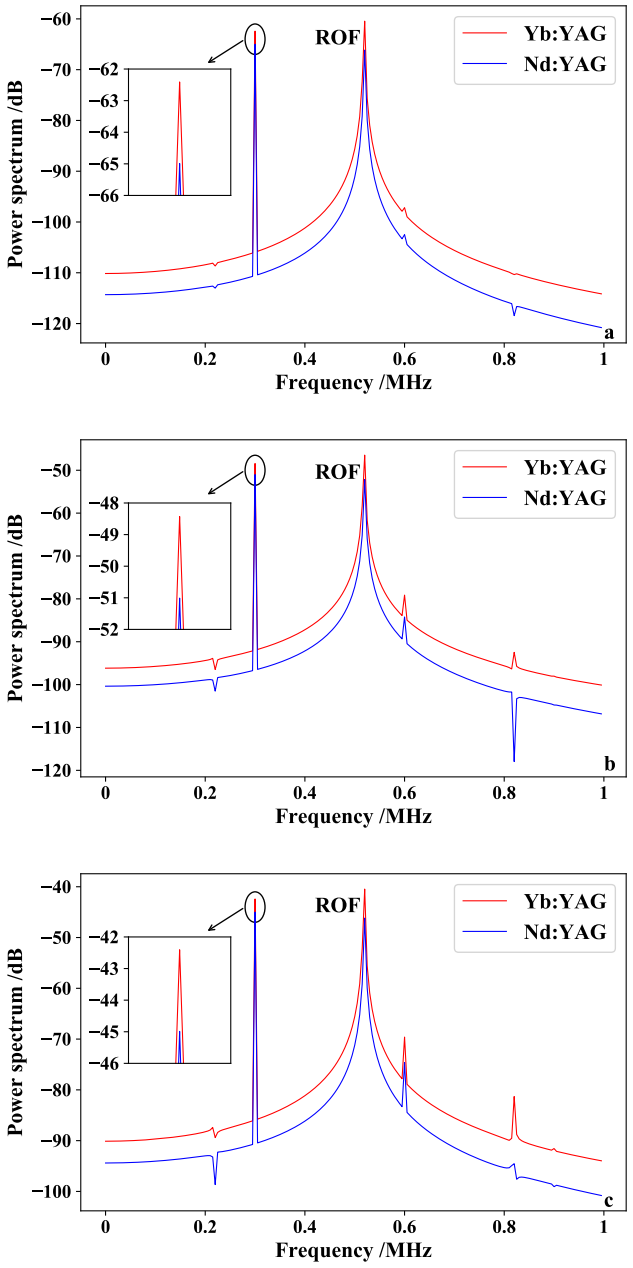

FIGURE 1. Power spectra of the Yb:YAG and Nd:YAG SSLs. (a: $\gamma_{ext} = 1 \times 10^{-6}$; b: $\gamma_{ext} = 5 \times 10^{-6}$; c: $\gamma_{ext} = 1 \times 10^{-5}$.)

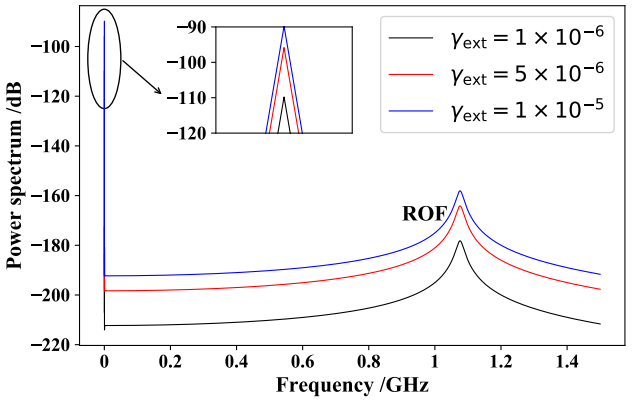

FIGURE 2. Power spectrum of the LD.

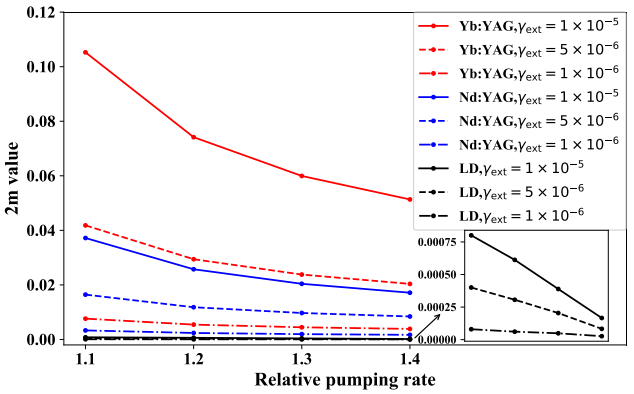

FIGURE 3. Simulative 2*m* values of three laser types under different conditions.

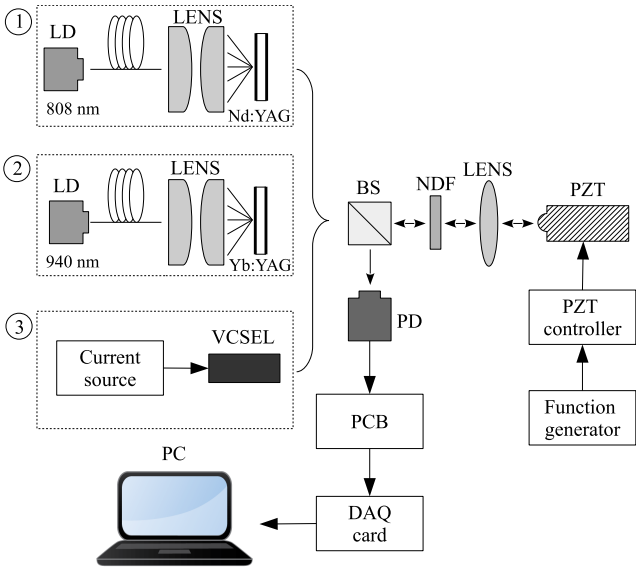

FIGURE 4. Experimental setup.(LD: Laser diode; VCSEL: Vertical cavity surface emitting laser; BS: Beam splitter; NDF: Neutral Density Filter; PZT: Piezoelectric transducer; PD: Photodiode; DAQ: Data acquisition).

high voltage piezoelectric controller (Thorlabs, MDT694B). The external signal comes from a function generator, making the PZT vibrating in sinusoidal waveforms with the frequency of 100Hz or 200Hz (upper bound of the bandwidth of the PZT) and the amplitude varying from 1.5 μm to 4.5 μm during the whole experiment. Sinusoidal waveforms are utilized here as they are the fundamental components of any kind of vibration, and the instantaneous Doppler frequency is easily calculated to be less than 10 kHz as mentioned in section II-B. The signal conditioning circuit only has a current-to-voltage converter, without any amplifying or filtering, to maintain the signals' original waveform. The trans-impedance gain of the circuit is not that significant in this study since it has the same effect on both the DC and AC components of SMI signals and will be canceled as shown in Eq. (8). All the SMI signals

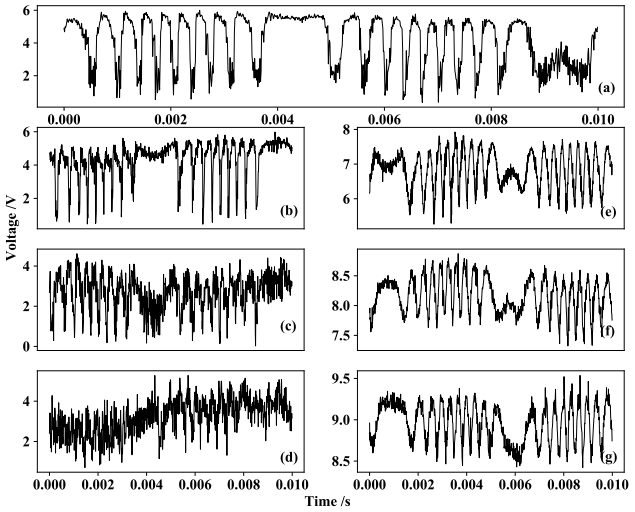

FIGURE 5. SMI signals of the Nd:YAG laser for example at 3 μm 100 Hz vibration.[(a). $I_p = 1.1$ A without the NDF; (b). $I_p = 1.1$ A with the NDF at position 1; (c). $I_p = 1.1$ A with the NDF at position 2; (d). $I_p = 1.1$ A with the NDF at position 3; (e). $I_p = 1.2$ A without the NDF; (f). $I_p = 1.3$ A without the NDF; (g). $I_p = 1.4$ A without the NDF.)]

are sampled through a data acquisition card (USB-61902, JYTEK, China) to a PC for subsequent calculation which also depends on Python 3.7.

First of all, some exemplar SMI signals acquired from experiments are presented in the following Fig. 5, and only those of the Nd:YAG laser are shown just because different laser types have similar SMI fringe shapes. Where I_p is the pumping current. Figs. 5(a) to 5(d) can be utilized to observe the influence of feedback level, as NDF positions 1, 2 and 3 have decreasing transmittance, and Figs. 5(a), 5(e), 5(f) and 5(g) can be used to explore the impact of pumping level.

Here, the peak-to-peak value $2m$ is utilized for comparison without the NDF, which is demonstrated in Fig. 6. Considering nearly linear relation between current and power in LDs, the pumping current values of three laser types are set to 1.2 times of the threshold current, which are 2.7 A for the Yb:YAG one, 1.2 A for the Nd:YAG one and 2.4 mA for the VCSEL. Under each vibration condition, totally ten segments are truncated from the SMI signal for evaluation, and each segment has 2000 data points. Where the horizontal tick labels are the PZT's vibration amplitude and frequency, the error bars are the results of ten times of calculations, and the dot is the mean value and the line segment is the standard deviation. As depicted in Fig. 6, SSLs always have pronouncedly larger signal amplitude than that of the LD under the same vibration condition, and between these two types of SSLs, the Yb:YAG's signal amplitude can be somewhat larger than that of the Nd:YAG, which coincides with the simulation results mentioned above.

Then, the influence of pumping power in SSLs or injection current in LDs are further discussed, as shown in Fig. 7. Considering the upper voltage bound of the sampling card is 10 V, the same relative pumping level (1.1, 1.2, 1.3 and

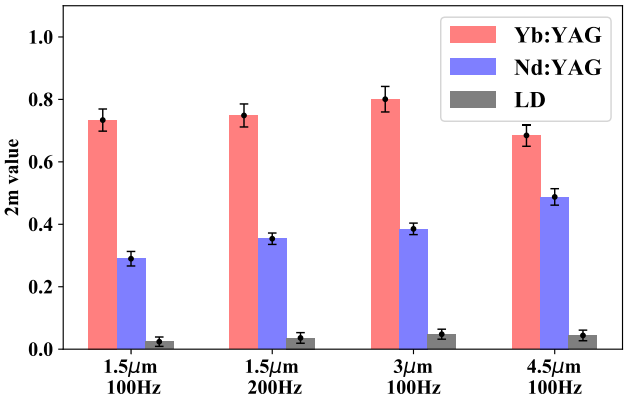

FIGURE 6. $2m$ values comparison under different vibration conditions, without the NDF and with the same pumping level.

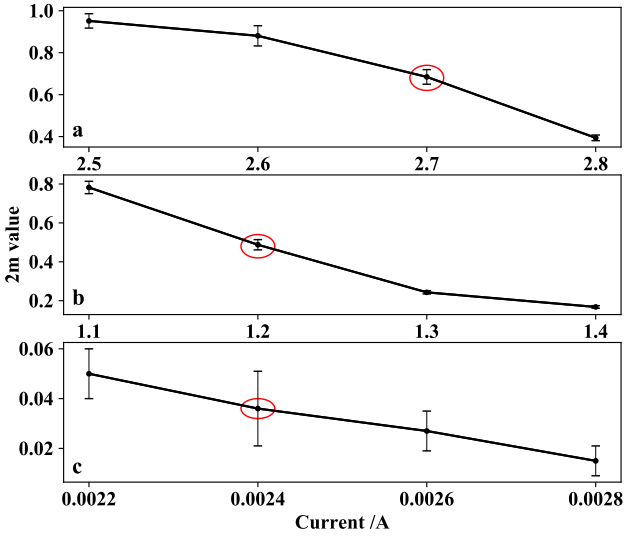

FIGURE 7. $2m$ values under 4.5 μm 100 Hz vibration, without the NDF and with different pumping or injection current values. (a: Yb:YAG; b: Nd:YAG; c: LD).

1.4 times the threshold current) can not be uniformly set for all three laser types. In the Yb: YAG laser, for example, 1.3 times the threshold current reaches 2.93 A, which will cause the corresponding SMI signal grow beyond 10 V and can not be sampled. Thus, four more suitable pumping current values are selected for the Yb:YAG laser to reflect the effect of the pumping level on the signal sensitivity. Where the error bars have the same meaning as in Fig. 6, and the points in the red circles correspond to the same pumping level of Fig. 6. Obviously, increasing pumping level indicates gradually decreasing signal sensitivity. It can be deduced that the highest sensitivity must occur around the pumping level just above the threshold.

Finally, the influence of feedback levels are discussed, and the results are depicted in Fig. 8. Three NDF positions with decreasing transmittance are marked and adopted to adjust the feedback level for three laser types. It can be concluded that a lower feedback level corresponds to lower signal sensitivity

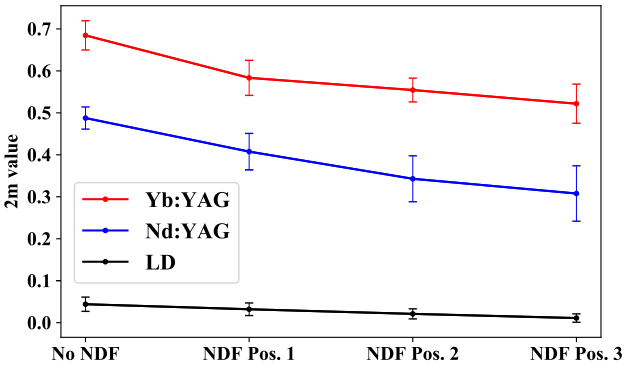

FIGURE 8. **2*m* values comparison under 4.5 μm 100 Hz vibration, with the same pumping level and different feedback levels.**

since noise starts to be more prominent if less laser beam coupled back into the cavity. In addition, SSLs are still more sensitive than the LD and the Yb:YAG is still more sensitivity than the Nd:YAG.

What is observed in Figs. 7 and 8 for each laser type highly accords with the conclusions published in literatures [21], [22], and all the experimental phenomena exhibited above agree well with the simulation results in the last section. Therefore, it can come to the conclusions that

- SSLs are more sensitive to laser feedback than LDs due to high FPLR, and the Yb:YAG laser is more sensitive than the Nd:YAG one.
- For SSLs or LDs, increasing the pumping level from the threshold will decrease the SMI signal's sensitivity.
- For SSLs or LDs, reducing laser feedback strength will also decrease the SMI signal's sensitivity.

IV. CONCLUSION

Considering detection sensitivity in SMI precision measurement, we compare the sensitivity performance of three laser types, including a Yb:YAG SSL, a Nd:YAG SSL and a LD. It can be verified through both the simulation based on perturbation rate equations and the experiment regarding the peak-to-peak value 2*m* that SSLs are more sensitive to laser feedback than LDs, and the Yb:YAG is more sensitive than the Nd:YAG. The phenomena may depend on the intrinsic parameter of laser materials, which is named FPLR. Larger FPLR values bring about higher SNR and larger 2*m* values. Additionally, increasing pumping level or decreasing feedback level means decreasing signal sensitivity. Therefore, instead of LDs, SSLs may be more suitable to be applied in the field of SMI precision measurement if miniaturization and cost are not the primary concerns, and what is proposed in the paper may provide guidance in developing high performance SMI sensors or instruments.

ACKNOWLEDGMENT

The authors would like to thank Dr. T. Lian for providing experimental instruments.

REFERENCES

[1] S. Donati and M. Norgia, "Overview of self-mixing interferometer applications to mechanical engineering," *Opt. Eng.*, vol. 57, no. 5, Mar. 2018, Art. no. 051506.

[2] Y. Ruan, B. Liu, Y. Yu, J. Xi, Q. Guo, and J. Tong, "Improving measurement sensitivity for a displacement sensor based on self-mixing effect," *IEEE Photon. J.*, vol. 10, no. 6, pp. 1–10, Dec. 2018.

[3] T. Taimre, M. Nikolić, K. Bertling, Y. L. Lim, T. Bosch, and A. D. Rakić, "Laser feedback interferometry: A tutorial on the self-mixing effect for coherent sensing," *Adv. Opt. Photon.*, vol. 7, no. 3, p. 570, Sep. 2015.

[4] J. Li, H. Niu, and Y. Niu, "Laser feedback interferometry and applications: A review," *Opt. Eng*, vol. 56, no. 5, May 2017, Art. no. 050901.

[5] K. Otsuka, "Self-mixing thin-slice solid-state laser metrology," *Sensors*, vol. 11, no. 2, pp. 2195–2245, Feb. 2011.

[6] S. Donati and M. Norgia, "Self-mixing interferometer with a laser diode: Unveiling the FM channel and its advantages respect to the AM channel," *IEEE J. Quantum Electron.*, vol. 53, no. 5, pp. 1–10, Oct. 2017.

[7] M. Usman, U. Zabit, O. D. Bernal, G. Raja, and T. Bosch, "Detection of multimodal fringes for self-mixing-based vibration measurement," *IEEE Trans. Instrum. Meas.*, vol. 69, no. 1, pp. 258–267, Jan. 2020.

[8] D. Guo, Y. Yu, L. Kong, W. Xia, and M. Wang, "Self-mixing grating interferometer with dual laser diodes for sensing of 2-D dynamic displacement," *IEEE J. Quantum Electron.*, vol. 54, no. 5, pp. 1–6, Oct. 2018.

[9] L. Lu, J. Yang, L. Zhai, R. Wang, Z. Cao, and B. Yu, "Self-mixing interference measurement system of a fiber ring laser with ultra-narrow linewidth," *Opt. Express*, vol. 20, no. 8, p. 8598, Apr. 2012.

[10] Z. Du, L. Lu, S. Wu, W. Zhang, B. Yang, R. Xiang, Z. Cao, H. Gui, J. Liu, and B. Yu, "Duplex self-mixing interference based on ultra-narrow linewidth fiber ring laser," *Opt. Commun.*, vol. 325, pp. 60–67, Aug. 2014.

[11] L. Shi, L. Kong, D. Guo, W. Xia, X. Ni, H. Hao, and M. Wang, "Note: Simultaneous measurement of in-plane and out-of-plane displacement by using orthogonally polarized self-mixing grating interferometer," *Rev. Sci. Instrum.*, vol. 89, no. 9, Sep. 2018, Art. no. 096113.

[12] K. Otsuka, K. Abe, J.-Y. Ko, and T.-S. Lim, "Real-time nanometer-vibration measurement with a self-mixing microchip solid-state laser," *Opt. Lett.*, vol. 27, no. 15, p. 1339, Aug. 2002.

[13] Y. Tan and S. Zhang, "Self-mixing interference effects of microchip Nd:YAG laser with a wave plate in the external cavity," *Appl. Opt.*, vol. 46, no. 24, p. 6064, Aug. 2007.

[14] Y. Tan, C. Xu, S. Zhang, and S. Zhang, "Power spectral characteristic of a microchip Nd:YAG laser subjected to frequency-shifted optical feedback," *Laser Phys. Lett.*, vol. 10, no. 2, Feb. 2013, Art. no. 025001.

[15] S. Zhang, S. Zhang, Y. Tan, and L. Sun, "A microchip laser source with stable intensity and frequency used for self-mixing interferometry," *Rev. Sci. Instrum.*, vol. 87, no. 5, May 2016, Art. no. 053114.

[16] Y. Zhao, S. Wu, R. Xiang, Z. Cao, Y. Liu, H. Gui, J. Liu, L. Lu, and B. Yu, "Self-mixing fiber ring laser velocimeter with orthogonal-beam incident system," *IEEE Photon. J.*, vol. 6, no. 2, pp. 1–11, Apr. 2014.

[17] A. A. Ibrahim, S. Ambran, F. Ahmad, O. Mikami, and C. Fujikawa, "Velocity measurement by self-mixing laser diode using direct modulation," in *Proc. IEEE 7th Int. Conf. Photon. (ICP)*, Apr. 2018, pp. 1–3.

[18] R. Lang and K. Kobayashi, "External optical feedback effects on semiconductor injection laser properties," *IEEE J. Quantum Electron.*, vol. QE-16, no. 3, pp. 347–355, Mar. 1980.

[19] Z. Zhang, C. Li, and Z. Huang, "Vibration measurement based on multiple Hilbert transform for self-mixing interferometry," *Opt. Commun.*, vol. 436, pp. 192–196, Apr. 2019.

[20] C. Kim, C. Lee, and O. Kwonhyok, "Effect of linewidth enhancement factor on fringe in a self-mixing signal and improved estimation of feedback factor in laser diode," *IEEE Access*, vol. 7, pp. 28886–28893, 2019.

[21] R. S. Matharu, J. Perchoux, R. Kliese, Y. L. Lim, and A. D. Rakić, "Maintaining maximum signal-to-noise ratio in uncooled vertical-cavity surface-emitting laser-based self-mixing sensors," *Opt. Lett.*, vol. 36, no. 18, p. 3690, Sep. 2011.

[22] J. Keeley, K. Bertling, P. L. Rubino, Y. L. Lim, T. Taimre, X. Qi, I. Kundu, L. H. Li, D. Indjin, A. D. Rakić, E. H. Linfield, A. G. Davies, J. Cunningham, and P. Dean, "Detection sensitivity of laser feedback interferometry using a terahertz quantum cascade laser," *Opt. Lett.*, vol. 44, no. 13, p. 3314, Jul. 2019.

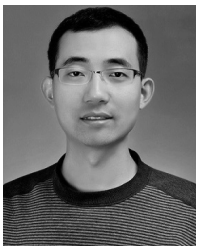

KE KOU was born in Shaanxi, China, in 1988. He received the B.S. degree in measurement and control technology and instrumentation and the M.S. and Ph.D. degrees in instrument science and technology from Tianjin University, in 2010, 2012, and 2016, respectively. He is currently working with the School of Mechanical and Precision Instrument Engineering, Xi'an University of Technology. His current research interests include laser self-mixing interferometry, solid-state lasers, and the application of machine learning in precision measurement.

CUO WANG was born in Hubei, China, in 1987. She received the B.S. degree in measurement and control technology and instrumentation from the Wuhan University of Technology, in 2010, and the M.S. and Ph.D. degrees in instrument science and technology from Tianjin University, in 2012 and 2016, respectively. She is currently working with the School of Mechanical and Precision Instrument Engineering, Xi'an University of Technology. Her current research interests include basilar membrane-based accelerometer, bionic sensing, and laser self-mixing interferometry.

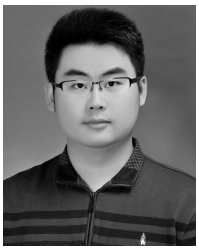

JUN WENG was born in Shaanxi, China, in 1988. He received the M.S. and Ph.D. degrees in precise instrument and mechanics from Northwestern Polytechnical University, in 2013 and 2017, respectively. He is currently working with the School of Mechanical and Precision Instrument Engineering, Xi'an University of Technology. His research interests mainly include gyroscope, inertial navigation, and integrated navigation.